Structure and Vibrational Properties of Sodium Disilicate Glass from ab Initio Molecular Orbital Calculations

Takashi Uchino* and Toshinobu Yoko

Institute for Chemical Research, Kyoto University, Uji, Kyoto 611, Japan

Received: March 19, 1998

We have carried out ab initio molecular orbital calculations on a cluster of atoms containing five $SiO_{3/2}O^-Na^+$ units connected at the corners by siloxane bonds to investigate the structure and vibrational properties of sodium disilicate glass. The optimized structural parameters (mean Si−O, O−O, and Na−O bond distances and O−Si−O bond angles) and O 1s photoelectron spectrum calculated at the Hartree−Fock/6-31G(d) level are in excellent agreement with the observed ones. We have also performed frequency calculations using the optimized cluster and have calculated their infrared and Raman intensities. The calculated vibrational spectra agree well with those observed for sodium disilicate glass. On the basis of the calculated results, we interpret the vibrational spectra of sodium disilicate glass and discuss the local coordination environments of sodium ions in the glass.

1. Introduction

The effects of alkali oxide on the structure of silicate glasses have been extensively studied for many years, since a large number of commercial silicate glasses contain alkali oxides, which dramatically affect various properties of glasses such as viscosity, thermal expansion, optical and electrical properties, and chemical resistance.[1] It is well accepted that alkali oxides incorporated into silica glass break up the Si−O−Si network to yield nonbridging oxygens (O_{nb}). The alkali cations adjacent to nonbridging oxygens are called the network-modifying cations. The formation of nonbridging oxygens will have the most crucial influence on the structure and the properties of alkali-containing glasses, and therefore, knowledge of the structure of alkali silicate glasses can be deduced from the distribution of silicons with various numbers of nonbridging oxygens.

Raman[2] and ^{29}Si nuclear magnetic resonance (NMR) spectroscopies[3−7] have been widely used to determine the distribution of silicate tetrahedra with *n* bridging oxygens, labeled often as "Q^n" ($0 \le n \le 4$). It has previously been shown that the structure of alkali silicate glasses can be understood in terms of the "binary" Q^n distribution model.[3,5,6] That is, as the alkali cations (R_2O) are added into SiO_2 glass, Q^3 units will be continually formed from Q^4 units, and the process continues until all Q^4 units are converted into Q^3 units at 33 mol % R_2O. Upon further addition of R_2O, Q^2 units will newly be formed at the expense of Q^3 units until all Q^3 units become exhausted at 50 mol % R_2O. However, recent ^{29}Si NMR studies have shown that the observed spectra should be interpreted in terms of the coexistence of several different Q^n species even at stoichiometric compositions; the fraction of the Q^4 or Q^2 structural unit in sodium disilicate glass has been reported to be 6−8%.[4,7]

In contrast to the knowledge about the distribution of Q^n species, a unified picture of the distribution and the coordination environments of the alkali cations in silicate glasses has not yet been obtained. Previous X-ray diffraction[8] and extended X-ray absorption fine structure (EXAFS) studies[9,10] on sodium silicate glasses have demonstrated that about five oxygen atoms are analyzed at a distance of 2.3−2.4 Å from one sodium atom. Such multiple coordination of Na is only possible with the help of both bridging (O_b) and nonbridging oxygen atoms. Although the Na−O_b bonds are expected to be longer than the Na−O_{nb} bonds, previous experimental techniques cannot differentiate these two kinds of Na−O bonds. It should also be noted that one observes relatively large changes in the chemical shifts for ^{29}Si and ^{23}Na NMR spectra between sodium silicate glasses and the corresponding crystals,[11] suggesting that there are substantial differences in the local environment of the sodium ions and that the coordination environments of alkali cations in glasses cannot be deduced simply from those of the corresponding crystals.

Recently, various quantum mechanical calculations have been increasingly useful in the field of glass structural science and hence can be regarded as alternatives to experimental approaches. In particular, ab initio molecular orbital (MO) methods have been widely used to calculate the theoretical geometries, bond energy, and vibrational properties of glassy systems.[12−16] In previous papers,[15] we have carried out ab initio MO calculations on a cluster of atoms modeling the local structure of alkali silicate glasses to obtain information about their local and electronic structures. We have calculated photoionization, X-ray emission, and ultraviolet (UV) excitation energies from the molecular orbital diagrams obtained for the model clusters and have found that the calculated energies are in good agreement with the experimental values of the corresponding real glassy systems. However, our previous models would be too small to analyze the local coordination environment of alkali cations in silicate glasses, since they consisted of two Q^n units, in which respective alkali cations are in contact only with one adjacent nonbridging oxygen atom.

To estimate alkali coordination environments in silicate glasses, we here employ a much larger cluster consisting of five $SiO_{3/2}ONa$ units. As will be shown below, this cluster indeed reproduces a multiple coordination of Na^+ ions and can hence provide a reasonable structural model of sodium silicate glasses on the medium-range length scale. Furthermore, we

* To whom correspondence should be addressed. E-mail: uchino@scl.kyoto-u.ac.jp. Fax: +81-774-33-5212.

10.1021/jp981564g CCC: $15.00
Published on Web 10/02/1998

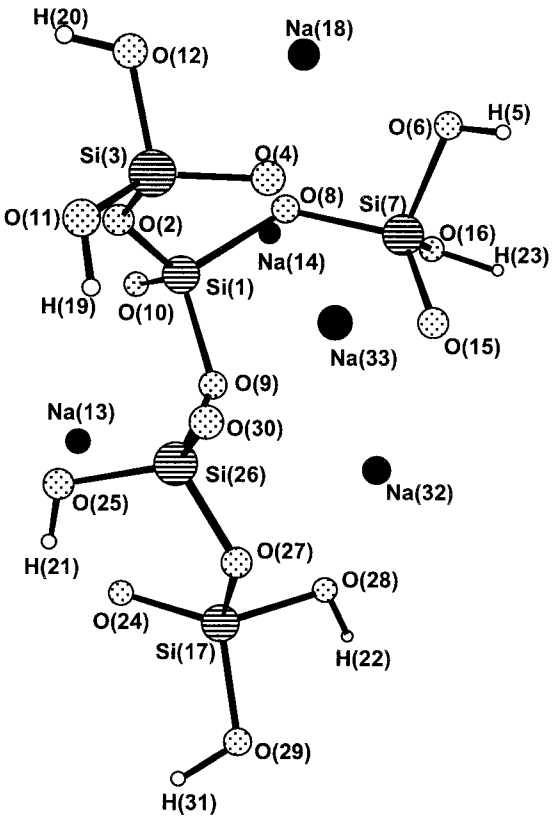

Figure 1. Optimized geometry of the cluster modeling the local structure of sodium disilicate glass calculated at the HF/6-31G(d) level.

calculate photoionization energies and harmonic vibrational frequencies of the model cluster and interpret the observed X-ray photoelectron (XPS) and vibrational spectra of alkali silicate glasses on the basis of the calculated results.

2. Models and Calculational Procedure

As mentioned above, we employed here a sodium silicate cluster containing five $SiO_{3/2}O^-$ units connected at the corners by siloxane (Si−O−Si) bonds (see Figure 1); each $SiO_{3/2}O^-$ unit has one Na^+ ion as a charge-compensating cation. This cluster can be compared to the local structure of $Na_2O{\cdot}2SiO_2$ glass, since, as mentioned in the Introduction, the Q^3 unit is the dominant structural unit in sodium disilicate glass. The "surface" oxygen atoms were terminated by H atoms to satisfy valences. The geometry of the model cluster was completely optimized at the Hartree−Fock (HF) level with the 6-31G(d) split-valence basis set.[17] Using the optimized geometry, we then performed a normal-mode analysis and obtained their harmonic frequencies. Force constants were obtained by the gradient methods,[18] and Raman scattering activities were calculated according to the procedure of Frisch et al.[19]

All ab initio MO calculations in this work were carried out using the Gaussian 94 computer program[20] on the CRAY T94/4128 supercomputer.

3. Results

Optimized Geometry. Figure 1 depicts the optimized geometry of the model cluster calculated at the HF/6-31G(d) level. Principal bond distances and bond angles are listed in Tables 1−3. We see from Table 2 that average Si−O and O−O bond distances calculated for the model cluster agree well with the observed ones.[21] Recently, we have calculated the optimized geometry of the cluster composed of nine $SiO_{4/2}$ units modeling the local structure of SiO_2 glass at the HF/6-31G(d) level,[22] and the average Si−O bond distance was calculated to be 1.622 Å. This value is shorter than that calculated for the present cluster (1.637 Å) by 0.015 Å. This is in good agreement with the observed tendency that the Si−O bond distance increases from 1.613 Å for amorphous silica to 1.631 Å for sodium disilicate glass.[21] One also notices from Table 1 that the average $Si-O_b$ bond distance (1.663 Å) of the present model cluster is longer than the average $Si-O_{nb}$ bond distance (1.560 Å) by about 0.1 Å. Vedishcheva et al.[23] previously reported that the Si−O peak of the neutron radial distribution function of sodium silicate glasses can be deconvoluted into two separate peaks due to the $Si-O_b$ (1.636 Å) and $Si-O_{nb}$ (1.587 Å) bonds, which are in reasonable agreement with our calculated results. These experimental and calculated results show that as alkali cations are incorporated into the SiO_2 structure the $Si-O_b$ and $Si-O_{nb}$ bond distances are increased and decreased, respectively, resulting in a longer mean Si−O bond distance than that in silica glass.

It should also be worth mentioning that the average Na−O distance calculated for the present model cluster is in good agreement with the experimental value[8−10,21] (see Table 2), although, as shown in Figure 1, the Na^+ ions in the model cluster are in contact with three to four oxygen neighbors, which is somewhat smaller than the observed coordination number of around five.[8−10] This discrepancy may be due to the open structure of the present model cluster. However, as will be

TABLE 1: Optimized Si−O Bond Distances and Si−O Bond Overlap Populations of the Model Cluster Calculated at the HF/6-31G(d) Level[a]

	bond distances (Å)	overlap populations
Si(1)−O(2)	1.615	0.691
Si(1)−O(8)	1.690	0.425
Si(1)−O(9)	1.643	0.503
Si(1)−O(10)	1.576	0.820
Si(3)−O(2)	1.666	0.515
Si(3)−O(4)	1.570	0.720
Si(3)−O(11)	1.627	0.752
Si(3)−O(12)	1.679	0.580
Si(7)−O(6)	1.676	0.560
Si(7)−O(8)	1.635	0.523
Si(7)−O(15)	1.555	0.903
Si(7)−O(16)	1.693	0.528
Si(17)−O(24)	1.555	0.950
Si(17)−O(27)	1.660	0.525
Si(17)−O(28)	1.695	0.487
Si(17)−O(29)	1.646	0.733
Si(26)−O(9)	1.696	0.334
Si(26)−O(25)	1.655	0.573
Si(26)−O(27)	1.668	0.481
Si(26)−O(30)	1.545	0.988
average $Si-O_b$[b]	1.663	0.547
average $Si-O_{nb}$	1.560	0.876

[a] Bond overlap populations are obtained from a Mulliken population analysis. for atom labels, see Figure 1. [b] O_b means both (Si−)O(−Si) and (Si−)O(−H) atoms.

TABLE 2: Optimized Si−O, O−O, and Na−O Bond Distances and Si−O−Si and O−Si−O Bond Angles (Averaged Values) of the Model Cluster Calculated at the HF/6-31G(d) Level[d]

	bond distances (Å)			bond angles (deg)	
	Si−O	O−O	Na−O	Si−O−Si	O−Si−O
calcd	1.637	2.670	2.376	131.7	109.2
obsd	1.631[a]	2.66[a]	2.4,[a] 2.35,[b] 2.30[c]		109.5[a]

[a] Reference 21. [b] Reference 8. [c] References 9 and 10. [d] Observed values for sodium disilicate glass are shown.

TABLE 3: Optimized Na−O Bond Distances and Na−O Bond Overlap Populations of the Model Cluster Calculated at the HF/6-31G(d) Level[a]

	bond distances (Å)	overlap populations
Na(13)−O(9)	2.641	0.069
Na(13)−O(10)	2.279	0.203
Na(13)−O(24)	2.176	0.256
Na(13)−O(25)	2.731	0.152
Na(14)−O(8)	2.365	0.113
Na(14)−O(10)	2.208	0.262
Na(14)−O(16)	2.391	0.144
Na(18)−O(4)	2.169	0.228
Na(18)−O(6)	2.382	0.146
Na(18)−O(8)	2.687	0.077
Na(18)−O(12)	2.520	0.142
Na(32)−O(9)	2.497	0.110
Na(32)−O(15)	2.220	0.197
Na(32)−O(27)	2.389	0.241
Na(32)−O(28)	2.267	0.157
Na(33)−O(4)	2.165	0.203
Na(33)−O(15)	2.471	0.162
Na(33)−O(30)	2.220	0.284
average Na−O_b[b]	2.487	0.135
average Na−O_{nb}	2.239	0.224

[a] Bond overlap populations are obtained from a Mulliken population analysis. For atom labels, see Figure 1. [b] O_b means both (Si−)O(−Si) and (Si−)O(−H) atoms.

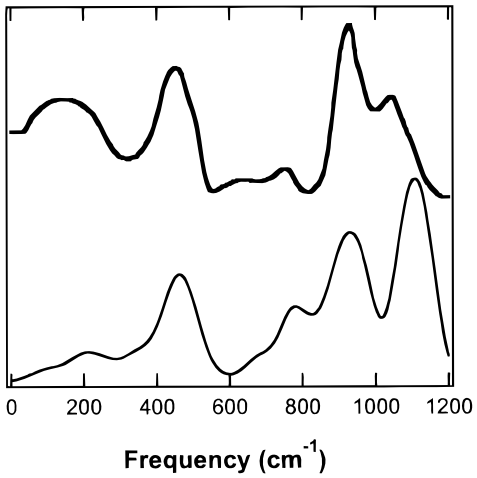

Figure 2. Calculated infrared absorption spectrum of the model cluster (bottom). The observed dielectric loss function of sodium disilicate glass (top, ref 36) is also shown.

shown below, the present MO calculations can reproduce various spectroscopic data such as XPS and vibrational spectra. It is then probable that the present model cluster represents some fundamental features of Na coordination environments and can be regarded as a reasonable model of actual sodium silicate glasses. In a later section, we will discuss the local coordination environments of Na^+ ions in more detail.

Infrared and Raman Spectra. We performed the HF/6-31G(d) vibrational analysis using the cluster optimized at the same level of theory mentioned above.[24] It is generally accepted that single-determinant wave functions yield too steep a potential in the vicinity of the equilibrium structure and that the theoretical frequencies at the HF level are consistently larger than the experimental harmonic quantities by ~10%.[25] We, therefore, used uniformly scaled frequencies to simulate vibrational spectra. We employed a value of 0.93 as the scaling factor, since the calculated frequencies multiplied by 0.93 gave the best correspondence with the observed frequencies. Figures 2 and 3 show the calculated smeared-out infrared and Raman spectra, respectively; both of the calculated spectra were convoluted with

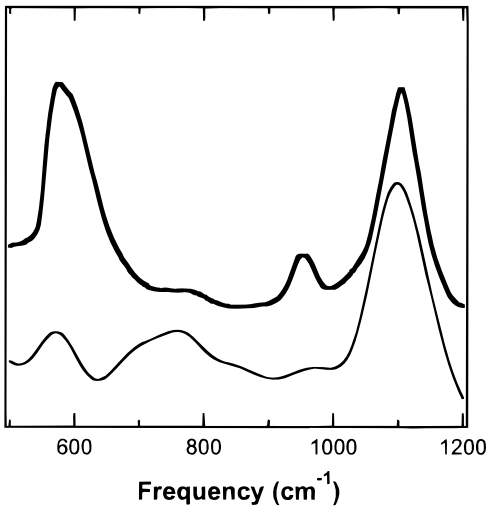

Figure 3. Calculated Raman spectrum of the model cluster (bottom). The observed Raman spectrum of sodium disilicate glass (top, ref 32) is also shown.

the use of Gaussian of width $\sigma = 33$ cm^{-1}. In Figures 2 and 3, we did not take into account the vibrational modes whose reduced masses m are smaller than 2 amu, since they are due mainly to the motions of surface H atoms and can be considered as artifacts caused by hydrogen terminations.

We see from Figures 2 and 3 that the main features of the observed infrared and Raman spectra of sodium disilicate glass are reasonably reproduced by the present frequency calculations, although there exists a slight discrepancy between the calculated and observed intensities. In section 4, we will discuss what types of vibrational motions contribute to these infrared and Raman bands.

O 1s XPS Spectrum. In previous papers,[15] we calculated the O 1s photoelectron energies of bridging and nonbridging oxygen atoms in alkali silicate glasses using clusters of atoms consisting of two SiO_4 tetrahedral units. We have shown that characteristic chemical shifts between the O 1s photoelectron lines of O_b and O_{nb} atoms in sodium silicate glasses can be reproduced by these calculations. In this work, we further calculate the O 1s XPS spectrum of the present model cluster by assuming a Gaussian−Lorentzian sum function for each photoelectron energy and compare directly the calculated spectrum with the observed one.

We calculated the O 1s photoelectron energies according to Koopmans' theorem,[26] which equates the photoelectron energy to the negative value of the one-electron energy of the corresponding orbital. To calculate the O 1s XPS spectrum, we employed a Gaussian−Lorentzian sum function f for each O 1s photoelectron energy, since such a sum function is often used to deconvolute the observed O1s XPS spectra.[27] This sum function is expressed by[28]

$$f = Cf_G + (1 - C)f_L$$

where C is the fraction of the Gaussian component,

$$f_G = \exp\left(-\ln 2\left(\frac{2(x-a)}{b}\right)^2\right), \quad f_L = \left(1 + \left(\frac{2(x-a)}{b}\right)^2\right)^{-1}$$

a is the calculated photoelectron energy, and b is the full width at half-maximum. We used 0.85 and 0.75 eV as values of C and b, respectively, and the resultant convoluted spectrum is shown in Figure 4. We see from Figure 4 that the spectral feature of the observed XPS spectrum[29] is satisfactorily

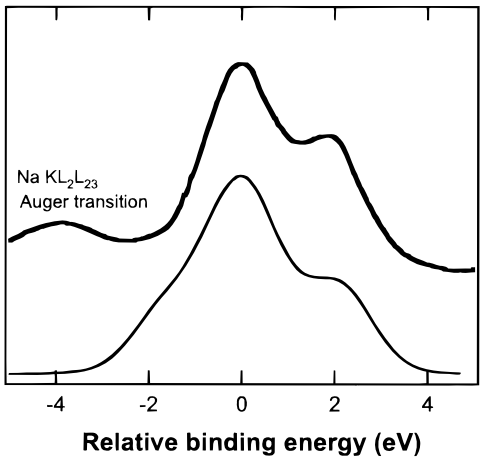

Figure 4. Calculated O 1s XPS spectrum of the model cluster (bottom). The observed O 1s spectrum of $0.3Na_2O{\cdot}0.7SiO_2$ glass (top, ref 29) is also shown. Kinetic energy scale is relative to the energy of the bridging oxygen atoms.

reproduced by the calculations; in particular, the calculated energy difference between O_b and O_{nb} atoms (~2.3 eV) is in excellent agreement with the observed one. We thus consider that the electronic structures of both bridging and nonbridging oxygen atoms in sodium silicate glasses can be described satisfactorily by the present MO calculations.

4. Discussion

Local Coordination Environments of Na Atoms. We have shown that ab initio cluster model calculations on the present model cluster can reproduce various spectroscopic data (infrared, Raman, and XPS) of sodium disilicate glass. It is then reasonable to assume that the structural model depicted in Figure 1 is basically consistent with the structure of actual sodium disilicate glass; the present model is certainly useful for a better understanding of the local coordination environments of Na in silicate glasses.

One notices from Table 3 that the distances of the $Na-O_{nb}$ bonds are generally shorter than those of the $Na-O_b$ bonds, indicating that the former bonds will be stronger than the latter ones. Furthermore, the $Na-O_{nb}$ bond overlap populations are considerably large in comparison with the $Na-O_b$ bond overlap populations (see also Table 3); that is, there exist strong covalent interactions between Na and O_{nb} in addition to the Coulomb forces. It is also interesting to note that each nonbridging oxygen atom in the present cluster tends to interact with more than one Na^+ ion (1.6 on average). Consequently, some Na^+ ions are coordinated by two to three nonbridging oxygens. Similar results have been also obtained from previous molecular dynamics simulations on the structure of alkali silicate glasses.[23,30] These results strongly suggest that the first neighbor coordination environments around the sodium ions will be determined mostly by the position of nonbridging oxygens and that each sodium atom will tend to interact with as many nonbridging oxygens as possible because of a strong interaction between alkali cations and nonbridging oxygens.

In actual sodium disilicate glass, the coordination number of Na will be slightly larger than that obtained from the present cluster model. However, the above rule can be basically applied to the actual glasses. Thus, we consider that the glass network of sodium silicate glasses will be so constructed as to maximize the number of nonbridging oxygen atoms around Na^+ ions. As a result, the positive charge of Na^+ ions in the glass network will be most effectively compensated in the silicate network.

Interpretation of the Vibrational Spectra. Infrared and Raman spectroscopies have been extensively used to investigate the structure and vibrational properties of silicate glasses.[2,31,32] However, the precise assignments of the vibrational spectra of disordered systems are in general very difficult, and no accurate calculations of infrared and Raman intensities of sodium silicate systems have been reported. We hence interpret the observed vibrational spectra of sodium silicate glasses on the basis of the harmonic normal-mode frequencies calculated for the present cluster.

In the following discussion, we divide the vibrational spectra of sodium disilicate glass into three regions, namely, the high-frequency region (900−1200 cm^{-1}), the mid-frequency region (400−800 cm^{-1}), and the low-frequency region (100−300 cm^{-1}).

i. High-Frequency Region. The infrared and Raman spectra of sodium disilicate glass show two bands at 900−950 and 1050−1100 cm^{-1} in the high-frequency region. The strong infrared bands at 1050−1100 and 900−950 cm^{-1} have been attributed to Si−O stretching modes of the network-bound SiO_4 tetrahedron and nonbridging oxygens, respectively.[33] On the other hand, Raman spectroscopic studies have differently interpreted that the 1050−1100 and 900−950 cm^{-1} bands are associated with symmetric silicon−oxygen stretching motions of Q^3 and Q^2 units, respectively.[2] However, ^{29}Si NMR studies have demonstrated that Q^2 units hardly exist in low alkali silicate glasses (<33 mol %),[3] suggesting that the 900−950 cm^{-1} band should not be attributed to the motions of Q^2 units as far as low alkali silicate glasses are concerned.

To investigate the motions that are responsible for the 1050−1100 and 900−950 cm^{-1} bands, we here analyze the vector displacements for the vibrational modes of the present cluster in the high-frequency region (see Figure 5a−d). According to the normal coordinates calculated, we see that the vibrational modes in the frequency region at 1050−1100 cm^{-1} are due to the localized stretching motions of $Si-O_{nb}$ bonds in $SiO_{3/2}O^-$ units (see Figure 5a−c), in agreement with the interpretation derived from previous Raman studies.[2]

In contrast to the previous expectations, however, the vibrational modes in the frequency range at 900−950 cm^{-1} are not associated with the motions of O_{nb} atoms; we see from Figure 5d that these vibrational modes result from stretching motions of the $Si-O_b$ bonds in the Si−O−Si network. In infrared and Raman spectra of SiO_2 glass, such $Si-O_b$ stretching modes are located at 1000−1200 cm^{-1}.[2,33] Thus, one might consider that the present vibrational modes in the frequency region at 940−950 cm^{-1} are far from realistic. However, one should recall that the $Si-O_b$ bond distance is substantially elongated as sodium ions are added into the SiO_2 structure (see section 3). Such an elongation of the $Si-O_b$ bond distance certainly leads to a decrease in the force constants of $Si-O_b$ stretching modes, and accordingly, stretching vibrations of thus weakened $Si-O_b$ bonds in alkali silicate glasses will occur at lower frequencies than the corresponding $Si-O_b$ stretching modes in SiO_2 glass. We, therefore, consider that the 900−950 cm^{-1} band in sodium silicate glasses should be attributed to the stretching modes of the $Si-O_b$ bonds weakened by the addition of Na into the glass structure.

ii. Mid-Frequency Region. In the mid-infrared region, sodium silicate glasses show major vibrational bands at 400−600 and 700−800 cm^{-1}. It has been suggested that the 400−600 cm^{-1} band results from a highly delocalized vibrational mode of the silicate network to which both bridging and nonbridging oxygen bending motions contribute, whereas the

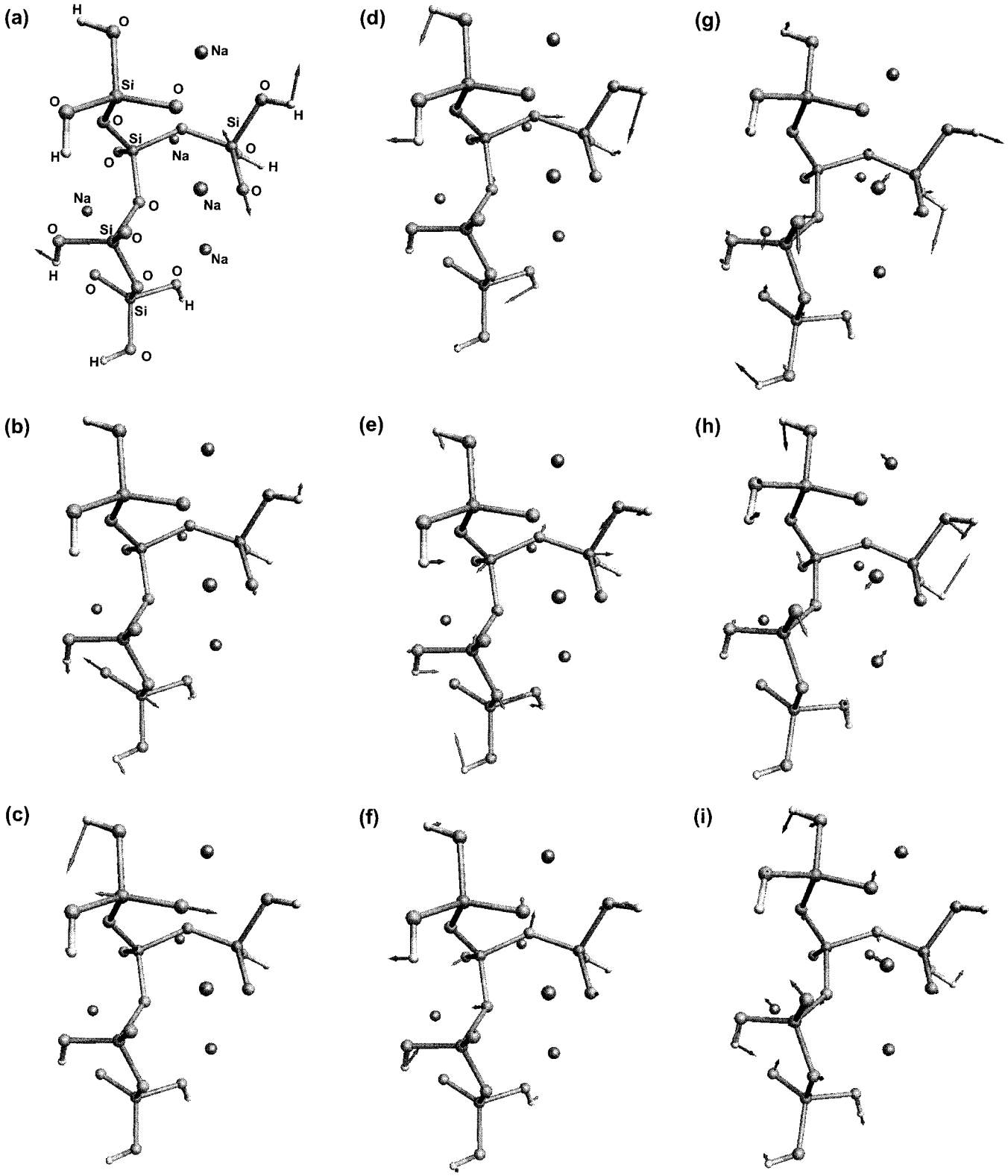

Figure 5. Vector displacements of the normal modes with scaled frequencies (scaling factor 0.93): (a) 1120, (b) 1104, (c) 1081, (d) 951, (e) 764, (f) 498, (g) 293, (h) 217, (i) 120 cm^{-1}.

700−800 cm^{-1} band is associated with motions of silicon against its tetrahedral cage.[2] We have found that these assignments are essentially in agreement with our calculations (for the 700−800 and 400−600 cm^{-1} bands; see parts e and f of Figure 5, respectively).

iii. Low-Frequency (Far-Infrared) Region. Since alkali cation vibrations in their equilibrium positions in oxide glasses can be observed in the frequency range below ∼400 cm^{-1}, far-infrared spectra of alkali oxide glasses have been extensively studied to get information about the cation−anionic site interactions.[35−37] The vibrational frequencies of Na^+ ions in silicate glasses are reported to be 200−250 cm^{-1}.[34,36] As shown in Figure 2, the present cluster model calculations satisfactorily reproduce the observed far-infrared band at ∼200 cm^{-1}. Normal coordinates of the principal far-infrared modes are depicted in Figure 5g−i. We see from Figure 5g−i that these far-infrared

modes indeed result from the motions of Na^+ ions. However, the vibrations of Na^+ ions also accompany the motions of nonbridging oxygens, indicating that the cation vibrations in their anionic sites are not completely decoupled from the vibrations of the glass network.

Kamitsos et al.[35,37] previously suggested that the broad asymmetric far-infrared bands seen in many inorganic glasses can be deconvoluted into two Gaussian type components, which are assigned to vibrations of alkali cations in two different distributions of cation−anionic site environments. However, such an interpretation has been recently questioned by us on the basis of the normal-mode analysis of some sodium borate clusters.[38] We have demonstrated that the asymmetric feature of the far-infrared bands of sodium borate glasses should be ascribed to the two types of vibrational modes between Na^+ and its charge-compensating BO_4^- unit; the lower- and higher-frequency components of the far-infrared bands are due to the $Na^+-BO_4^-$ bendinglike and stretchinglike motions, respectively. As for the present sodium silicate cluster, we have also found that the motions of each Na^+ atom contribute to the lower-frequency parts as well as to the higher-frequency parts of the vibrational modes below 300 cm^{-1} (see Figure 5 g−i), suggesting that the broad far-infrared bands of sodium silicate glasses result from the changes in the force constant of the alkali-motion modes in the respective alkali environments. The present results thus indicate that the cation motions in their ionic sites are not so simple as has been proposed by Kamitsos et al.[35,37] and, therefore, their "two-site model" should be reconsidered for a better understanding of the nature of far-infrared bands of oxide glasses.

5. Conclusions

We have performed ab initio molecular orbital calculations on a cluster of atoms modeling the local structure of sodium disilicate glass. The geometry of the cluster was completely optimized at the HF/6-31G(d) level, resulting in a multiple coordination of Na^+ ions that can be found in actual sodium disilicate glass. We have found that the $Na-O_{nb}$ bond distances are substantially shorter than the $Na-O_b$ bond distances. Furthermore, the bond overlap population of the $Na-O_{nb}$ bond is considerably larger than that of the $Na-O_b$ bond. Thus, the $Na-O_{nb}$ bonds are characterized by strong covalent interaction as well as Coulomb interaction. The first neighbor coordination environments of the sodium ions will hence be determined by the position of nonbridging oxygens; the glass network of sodium silicate glasses will be so constructed as to maximize the number of nonbridging oxygen atoms around Na^+ ions to compensate for the positive charge of Na^+ ions in the glass network most effectively. This rule probably explains why alkali cations and nonbridging oxygens tend to aggregate to form alkali rich regions in silicate networks.[30]

We have also carried out frequency calculations for the model cluster. The calculated infrared and Raman spectra of sodium disilicate glass were in reasonable agreement with the experimental spectra. On the basis of the normal coordinates, we propose a new interpretation for the 900−950 cm^{-1} band in sodium silicate glass; the band should be attributed to the stretching modes of the $Si-O_b$ bonds that are weakened by the addition of Na into the glass structure. Furthermore, we have found that the observed far-infrared band at ∼200 cm^{-1} is indeed due to the motions of Na^+ ions, although these cation vibrations in their anionic sites are not completely decoupled from the vibrations of the glass network.

Acknowledgment. We thank the Supercomputer Laboratory, Institute for Chemical Research, Kyoto University, for providing the computer time to use the CRAY T-94/4128 supercomputer. This work was partially supported by the Grant-in-Aid Scientific Research (09750922) from the Ministry of Education in Japan.

References and Notes

(1) See, for example, the following: Scholze, H. *Glass: Nature, Structure and Properties*; Springer-Verlag: New York, 1990.

(2) McMillan, P.; Piriou, B. *Bull. Mineral* **1983**, *106*, 57. McMillan, P. *Am. Mineral*. **1984**, *69*, 622.

(3) Stallworth, P. E.; Bray, P. J. *Glass-Science and Technology*; Uhlmann, D. R., Kreidl, N. J., Eds.; Academic Press: New York, 1990; Vol. 4B, pp 77−149.

(4) Duer, M. J.; Elliott, S. R.; Gladden, L. F. *J. Non-Cryst. Solids* **1995**, *189*, 107.

(5) Grimmer, A.-R.; Mägi, M.; Hähnert, M.; Stade, H.; Samonson, A.; Wieker, W.; Lippmaa, E. *Phys. Chem. Glasses* **1984**, *25*, 105.

(6) Dupree, R.; Holland, D.; Mortuza, M. G. *J. Non-Cryst. Solids* **1990**, *116*, 148.

(7) Murdoch, J. B.; Stebbins, J. F.; Carmichael, I. S. E. *Am. Mineral*. **1985**, *70*, 332. Stebbins, J. F. *Nature* **1987**, *330*, 465.

(8) Warren, B. E.; Biscoe, J. *J. Am. Ceram. Soc*. **1938**, *21*, 259.

(9) Greaves, G. N.; Fontaine, A.; Lagarde, P.; Raoux, D.; Gurman, S. J. *Nature* **1981**, *293*, 611.

(10) Greaves, G. N. *Glass-Science and Technology*; Uhlmann, D. R., Kreidl, N. J., Eds.; Academic Press: New York, 1990; Vol. 4B, pp 1−76.

(11) Dupree, R.; Holland, D.; McMillan, P. W.; Pettifer, R. F. *J. Non-Cryst. Solids* **1984**, *68*, 399.

(12) O'Keeffe, M.; Gibbs, G. V. *J. Chem. Phys*. **1984**, *81*, 876.

(13) Tossell, J. A.; Sághi-Szabó, G. *Geochim. Cosmochim. Acta* **1997**, *61*, 1171.

(14) Sykes, D.; Kubicki, J. D.; Farrar, T. C. *J. Phys. Chem. A* **1997**, *101*, 2715.

(15) Uchino, T.; Iwasaki, M.; Sakka, T.; Ogata, Y. *J. Phys. Chem*. **1991**, *95*, 5455. Uchino, T.; Sakka, T.; Iwasaki, M.; Ogata, Y. *J. Phys. Chem*. **1992**, *96*, 2455.

(16) Uchino, T.; Yoko, T. *J. Chem. Phys*. **1996**, *105*, 4140. Uchino, T.; Yoko, T. *Science* **1996**, *273*, 480.

(17) Hehre, W. J.; Ditchfield, R.; Pople, J. A. *J. Chem. Phys*. **1972**, *56*, 2257. Hariharan, P. C.; Pople, J. A. *Theor. Chim. Acta* **1973**, *28*, 213. Gordon, M. S. *Chem. Phys. Lett*. **1980**, *76*, 163.

(18) Pulay, P. *Mol. Phys*. **1969**, *17*, 197.

(19) Frisch, M. J.; Yamaguchi, Y.; Schaefer, H. F., III; Binkley, J. S. *J. Chem. Phys*. **1986**, *84*, 531.

(20) Frisch, M. J.; Trucks, G. W.; Schlegel, H. B.; Gill, P. M. W.; Johnson, B. G.; Robb, M. A.; Cheeseman, J. R.; Keith, T. A.; Petersson, G. A.; Montgomery, J. A.; Raghavachari, K.; Al-Laham, M. A.; Zakrzewski, V. G.; Ortiz, J. V.; Foresman, J. B.; Peng, C. Y.; Ayala, P. A.; Wong, M. W.; Andres, J. L.; Replogle, E. S.; Gomperts, R.; Martin, R. L.; Fox, D. J.; Binkley, J. S.; Defrees, D. J.; Baker, J.; Stewart, J. P.; Head-Gordon, M.; Gonzalez, C.; Pople, J. A. *Gaussian 94* Revision D.3; Gaussian, Inc.: Pittsburgh, PA, 1995.

(21) Misawa, M.; Price, D. L.; Suzuki, K. *J. Non-Cryst. Solids* **1980**, *37*, 85.

(22) Uchino, T.; Yoko, T. *Phys. Rev. B* **1998**, *58*, 5322.

(23) Vedishcheva, N. M.; Shakhmatkin, B. A.; Shultz, M. M.; Vessal, B.; Wright, A. C.; Bachra, B.; Clare, A. G.; Hannon, A. C.; Sinclair, R. N. *J. Non-Cryst. Solids* **1995**, *192&193*, 292.

(24) The vibrational analysis has yielded one imaginary frequency, indicating that the present optimized cluster is not true minimum. However, we did not carry out further geometry optimization using very precise convergence criterion, since the cluster has an extremely flat potential because of surface free OH groups and requires a lot of CPU time to get a true minimum structure.

(25) Hehre, W. J.; Radom, L.; Schleyer, P. v. R.; Pople, J. A. *Ab Initio Molecular Orbital Theory*; Wiley: New York, 1986; p 233.

(26) Koopmans, T. *Physica* **1933**, *1*, 104.

(27) Yamanaka, M.; Nakahata, K.; Terai, R. *J. Non-Cryst. Solids* **1987**, *95/96*, 405.

(28) Maddams, W. F. *Appl. Spectrosc*. **1980**, *34*, 245.

(29) Smets, B. M. J.; Lommen, T. P. A. *J. Non-Cryst. Solids* **1981**, *46*, 21.

(30) Huang, C.; Cormack, A. N. *J. Chem. Phys*. **1990**, *93*, 8180.

(31) Wong, J.; Angell, C. A. *Appl. Spectrosc. Rev*. **1971**, *4*, 155.

(32) Furukawa, T.; Fox, K. E.; White, W. B. *J. Chem. Phys*. **1981**, *75*, 3226.

(33) Crozier, D.; Douglas, R. W. *Phys. Chem. Glasses* **1965**, *6*, 240. Sweet, J. R.; White, W. B. *Phys. Chem. Glasses* **1969**, *10*, 246.

(34) Exarhos, G. J.; Risen, Jr., W. M. *Solid State Comm*. **1972**, *11*, 755. Exarhos, G. J.; Miller, P. J.; Risen, Jr., W. M. *J. Chem. Phys*. **1974**, *60*, 4145. Kamitsos, E. I.; Risen, Jr., W. M. *J. Non-Cryst. Solids* **1984**, *65*, 333.

(35) Kamitsos, E. I.; Chryssikos, G. D.; Karakassides, M. A. *J. Phys. Chem.* **1987**, *91*, 1067. Kamitsos, E. I.; Karakassides, M. A.; Chryssikos, G. D. *J. Phys. Chem*. **1987**, *91*, 5807. Kamitsos, E. I.; Patsis, A. P.; Chryssikos, G. D. *J. Non-Cryst. Solids* **1993**, *152*, 246.

(36) Merzbacher, C. I.; White, W. B. *Am. Mineral.* **1988**, *73*, 1089.

(37) Kamitsos, E. I. Yiannopoulos, Y. D.; Jain, H.; Huang, W. C. *Phys. Rev. B* **1996**, *54*, 9775. Kamitsos, E. I.; Chryssikos, G. D. *Solid State Ionics* **1998**, *105*, 75.

(38) Uchino, T.; Yoko, T. *Solid State Ionics* **1998**, *105*, 91.